SAND2018-12167J

Crystallization of electrically conductive visibly transparent ITO thin films by wavelength range specific pulsed Xe arc-lamp annealing

John B. Plumley[1,4], Adam W. Cook[2], Christopher A. Larsen[3], Kateryna Artyushkova[4], Sang M. Han[4], Thomas L. Peng[3], and Richard A. Kemp*[1,2]

1) Department of Chemistry & Chemical Biology, University of New Mexico, MSC03 2060, 300 Terrace St. NE, Albuquerque, NM 87131, USA
2) Advanced Materials Laboratory, Sandia National Laboratories, 1001 University Blvd. Albuquerque, NM 87106, USA
3) Space Vehicles Directorate, Air Force Research Laboratories, Kirtland Air Force Base, Albuquerque, NM, 87117, USA
4) Department of Chemical & Biological Engineering, MSC01 1120, 1 University of New Mexico, Albuquerque, NM, 87131, USA

*Corresponding author: E-mail: rakemp@unm.edu, Phone# (505)-277-6655

E-mail: JBP (john9@unm.edu); AWC (acook@sandia.gov); CAL (clarsen1@unm.edu); KA (kartyush@unm.edu); SMH (meister@unm.edu); TLP (AFRL.VSSVOrgMailbox@us.af.mil)

Abstract

Transparent electric conductors made of Indium Tin Oxide (ITO) doped glass prepared by a Flash Lamp Annealing (FLA) process are compared with ITO doped glass prepared via a conventional Rapid Thermal Annealing (RTA) process. Stylus surface profilometry was used to

determine thicknesses, scanning electron microscopy (SEM) was used to image surfaces, X-ray diffraction (XRD) was used to determine film structures, X-ray photoelectron spectroscopy (XPS) was used to determine oxidation states and film compositions, 4-point probe measurements were used to determine electrical conductivities, UV-Vis spectroscopy was used to determine film transparencies, and selective light filtering was used to determine which wavelengths of light are needed to anneal ITO into a visibly transparent electrically conductive thin film via an FLA process. The results show that FLA with visible light can be used to nearly instantaneously anneal ITO to create visibly transparent and electrically conductive ITO thin films on glass. The FLA process achieves this by predominately exciting unoxidized indium, unoxidized tin, tin monoxide (SnO), and non-stoichiometric indium oxide (InO_x), appropriately distributed in an electron beam physical vapor deposited (EBPVD) amorphous ITO thin film, to allow their oxidation and crystallization into an electrically conductive visibly transparent ITO. Though it is possible to prepare ITO doped glass that is more transparent with an RTA process, the FLA process is significantly faster, has comparable electrical conductivity, and can strongly localize heating to areas of the as deposited ITO thin film that are not electrically conductive and visibly transparent.

Keywords

Thin films; flash lamp annealing; rapid thermal annealing; indium tin oxide; resistivity; transparent conducting oxide

Introduction

Electrically conductive transparent materials are key components in a variety of devices such as electronic touch screens [1] and solar cells [2]. A common way to create such materials is to deposit and anneal a thin film of Transparent Conducting Oxide (TCO) on an electrically insulating transparent substrate. This imparts the electrically conductive properties of the TCO thin film, a film too fragile to stand alone, to the surface of the substrate, the transparency of which typically requires it to be non-conductive, without significantly attenuating the transparency of the underlying substrate with the often less transparent nature of the annealed TCO thin film. To establish this coating, raw constituents of the TCO are often deposited on the target substrate via a surface deposition technique such as ion beam assisted sputter deposition [3], Electron Beam Physical Vapor Deposition (EBPVD) [4], Chemical Vapor Deposition (CVD) [5], pulsed laser deposition [6], sol gel dip-coating [7], or colloidal solution spin coating [8]. Once deposited, these opaque and electrically insulating raw constituents are made electrically conductive and transparent by crystallizing these constituents with an annealing process. Effective annealing treatments include lengthy heating in a furnace [9] or Rapid Thermal Annealing (RTA) [10]. More recently, laser annealing [11] and Flash Lamp Annealing (FLA) [12, 13] have allowed near-instantaneous annealing of TCOs.

The short processing time and reduced thermal stress imposed on materials offered by the FLA process make it an attractive approach to preparing electrically conductive transparent materials. However, uncertainty in how the FLA process works limits the extent it can be improved or optimized for a specific application. In this study, a clearer understanding of the flash annealing process is achieved by determining how flash annealing EBPVD Indium Tin Oxide (ITO) with different bands of light affect the transparency and electrical conductivity of the resulting thin film relative to EBPVD ITO annealed via a conventional RTA process. The results suggest that the FLA process nearly instantaneously creates transparent conductors, comparable in quality to ones created via an RTA process, by predominately heating the visibly opaque and non-electrically conductive uncrystallized and incompletely oxidized regions of the unannealed ITO deposit.

Experimental

EBPVD of Unannealed ITO Thin Films

200Å, 300Å, 400Å, 500Å, and 600Å thick films of unannealed ITO were deposited on 2.5cm x 2.5cm x 0.1cm soda-lime glass substrates (VWR) by vaporizing ITO off 99.999% pure ITO granules (In_2O_3(90)/SnO_2(10) Wt% International Advanced Materials), placed in a graphite crucible, with a dielectric evaporator (CHA Mark 40). This ITO vapor was delivered to the target substrate by incorporating it into a static O_2 stream directed towards a substrate face. Note that the ITO target consisted of heat fused granules of In_2O_3, with the appropriate amount of SnO_2 distributed in it, such that vaporizing this target created a deposition stream that deposited the appropriate distribution of indium and tin on the target substrate to allow their crystallization and oxidation into the electrically conductive visibly transparent tin doped In_2O_3. Facilitating such chemical treatment, driven by thermal annealing, was needed as the polycrystalline and incompletely oxidized nature of the as deposited ITO film made it neither visibly transparent nor electrically conductive. Pressure in the deposition chamber, prior to initiating any gas flows, was measured to be 2.0×10^{-6} torr. Initiating the O_2 stream increased this pressure to 9.0×10^{-5} torr. ITO vaporization power was set at 3.1 kW. This established a 0.3 Å/sec ITO deposition rate. To compensate for idiosyncrasies in the rate of ITO impinging different areas of the substrate face, the target substrate was steadily moved while under the deposition stream in orbital motion during the deposition process. Total ITO deposition was monitored with a quartz crystal microbalance situated in the deposition chamber and the thickness of the ITO deposit was verified with a stylus surface profilometer (Bruker DektakXT).

RTA Annealing

RTA annealing of the EBPVD deposited ITO on glass substrates was performed under a N_2 flow with an RTA system (Process Products 1150). To complete the RTA process, samples placed in the RTA system were purged with N_2 for 2 minutes at 25°C. While maintaining the N_2

flow, the temperature in the RTA chamber was ramped from 25°C to 200°C at a rate of 1.5°C/sec, then held at 200°C for 2 minutes, then ramped from 200°C to 550°C at a rate of 0.6°C/sec, then held at 550°C for 10 minutes, and finally allowed to cool for 60 minutes to return to room temperature. The total time required to complete an optimized RTA process was around 74 minutes.

FLA Annealing

FLA annealing of the EBPVD deposited ITO on glass substrates was performed under a N_2 flow with a photonic curing system (NovaCentrix PulseForge 1300). To complete a single FLA treatment, samples were positioned 22mm away from a Xe arc lamp with the face of the ITO deposit directed towards the incident light. This light consisted of a 2200μs pulse envelope comprised of eight 200μs pulses of blackbody radiation, extending from 200nm to 1500nm, with a 75μs break after each pulse. The initial pulse intensity reached 35,000w/cm^2, the second pulse reached 26,000w/cm^2, the third reached 22,000w/cm^2, the fourth reached 18,000w/cm^2, the fifth reached 15,000w/cm^2, the sixth reached 12,000w/cm^2, the seventh reached 10,000w/cm^2, and the final pulse reached 8,000w/cm^2. Repeating the FLA treatment can improve the electrical conductivity and visible transparency of the FLA treated ITO, but there was no noticeable improvements after 10 treatments. Reapplications of the FLA treatment can be applied immediately after a prior treatment without waiting for the FLA treated sample to cool. The FLA samples discussed in this report were all prepared with an FLA process, consisting of 20 sequential flash lamp treatments, with the exception of the tests shown in Figure 8 where the number of treatments applied in the FLA process was varied. The total time required to complete an FLA process consisting of 20 FLA treatments followed by a brief cooldown period after the final FLA treatment was around 20 seconds.

Materials Characterization

Stylus surface profilometry (Bruker DekTakXT) was used to determine film thicknesses. X-Ray Diffraction (Rigaku Smartlab XRD) was used to determine the crystallinity of films. The

sheet resistance of prepared samples was determined with a Lucas Labs Pro 4 probe paired with a Keithley 2400 SourceMeter. X-ray Photoelectron Spectroscopy (Krato AXIS Ultra XPS) was used to track changes in metal oxidation states and thin film compositions. UV-Vis spectroscopy (Perkin Elmer Lambda 950 UV/VIS/IR) and a HeNe laser setup (Thorlabs HNL020L laser paired with a Thorlabs PM204 power meter) were used to evaluate the optical properties of deposits and their compositions. Scanning Electron Microscopy (Hitachi S-4300 SE SEM) was used to image ITO deposits and, finally, bandpass filters were used to determine which wavelengths emitted by the Xe-arc lamp during the FLA treatments drove the desired annealing processes. The soda-lime glass substrates which ITO was deposited on in this study transmitted light from 350nm to 2000nm. A cerium oxide band pass filter (NovaCentrix) was used to block UV light by absorbing wavelengths shorter than 425nm. A hot mirror (Edmund Optics) was used to block IR light by reflecting wavelengths from 750nm to 1500nm and transmitting light from 425nm to 675nm. A cold mirror (Edmund Optics) was used to block visible light by reflecting wavelengths from 425nm to 675nm and transmitting light from 800nm to 1200nm.

Results and Discussion

Oxides deposited using EBPVD undergo reduction to form oxygen deficient visibly opaque films[14]. As shown in Figure 1, EBPVD of ITO onto a glass surface establishes a dark gray deposit that becomes visibly transparent after FLA or RTA processing. Figure 1a shows 200Å of the dark grey unannealed vapor deposited ITO on glass. The clear trapezoid on the“as deposited” sample stems from the clip used to hold the glass substrate during the EBPVD procedure. This clip blocked impinging gases and kept vaporized ITO from adhering to the area of glass under the clip. Figure 1c shows 200Å of the as deposited ITO on glass after it was annealed by an RTA process. Note that visible inspection finds that annealed ITO was as transparent as the blocked trapezoidal area where no deposit was established. Figure 1b shows 200Å of the deposit after a circular area of it was flash annealed. Here, examining the trapezoidal area where the clip blocked deposition shows that the FLA process created a transparent thin film; however, this film was not as transparent as the film created by RTA.

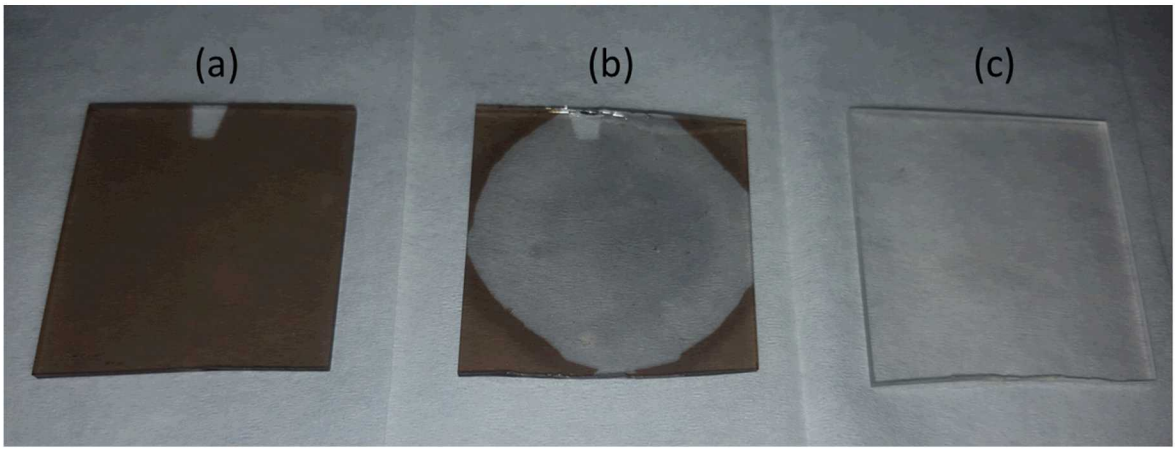

Fig. 1 200Å of ITO deposited onto a glass substrate (a) as deposited, (b) after FLA treatment in a circular area, and (c) after RTA treatment

As shown in Figure 2, the lack of diffraction angle (2θ) peaks in the XRD spectra of the unannealed deposit indicates that this deposit is completely amorphous. The appearance of 2θ peaks in the XRD spectra of the FLA and RTA treated deposits confirm that both these processes induce grain growth within the amorphous material. The presence of the amorphous halo for the XRD lines of the annealed samples indicates that the annealed films are polycrystalline or still nearly amorphous but with small grains embedded in the amorphous material. The amorphous halo is also likely attributed to the glass substrate. The slightly higher intensity of the XRD peaks from the RTA treated samples indicates that RTA is more effective at crystallizing amorphous ITO than the FLA process. The FWHM of the de-convoluted (222) peak is 0.46 for RTA treated ITO and 0.70 for FLA treated ITO. The slightly broader FLA peak indicates that the FLA treated ITO may have smaller grains than that of the RTA sample. Additionally, the diffraction angles at which these XRD peaks appear, and their relative intensities, indicate that the grains in the annealed films have primarily an In_2O_3 crystal structure [15]. However, the peaks are much smaller and less distinguished than that of previously reported XRD spectrum for powder ITO [16].

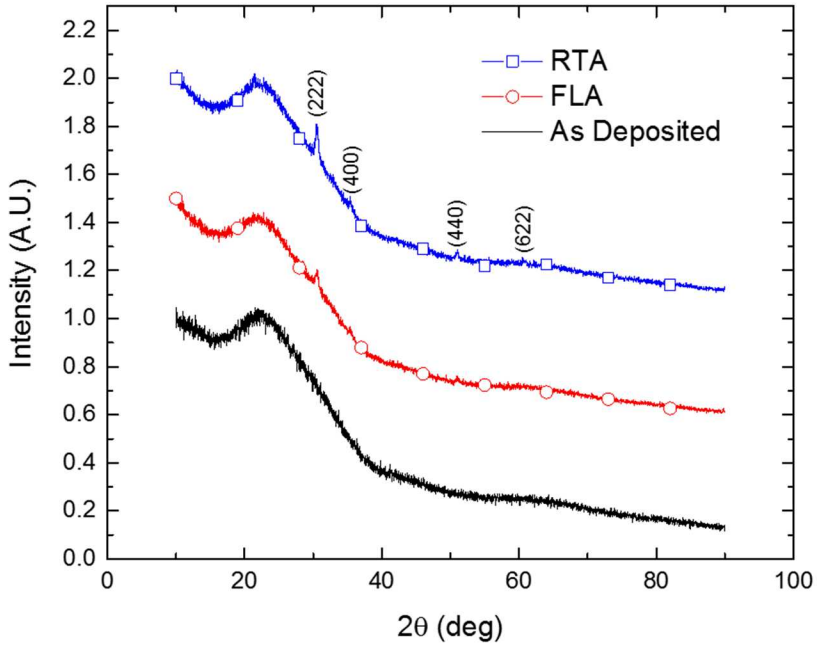

Fig. 2 XRD Spectra for 200 Å of ITO on glass substrates for as deposited ITO as well as RTA and FLA processed ITO samples

XPS data of the ITO deposits, before and after annealing, indicate that the thin films were composed of completely oxidized indium oxide (In_2O_3), incompletely oxidized non-stoichiometric indium oxide (InO_x), unoxidized indium (In^{+0}), completely oxidized tin oxide (SnO_2), incompletely oxidized tin oxide (SnO), and unoxidized tin (Sn^{+0}). Referencing the NIST XPS database, lower binding energy peaks were attributed to unoxidized and incompletely oxidized metals [17]. Shown in Figure 3, the combined amount of incompletely oxidized InO_x and unoxidized In^{+0} in a deposit was indicated by the relative area percentage under the curve of the ~444eV binding energy peak. The extent to which indium in the thin film was in the +3 fully oxidized In_2O_3 state was indicated by the relative area percentage under the curve of the ~445eV binding energy peak to the ~444eV binding energy peak. As shown in Figure 3a, the ITO target granules have a significant amount of In_2O_3. After EBPVD, the low area percentage of the ~445eV peak relative to the ~444eV peak, shown in Figure 3b, indicates that much of the indium present in the amorphous as deposited thin film was reduced to partially oxidized non-stoichiometric InO_x and unoxidized In^{+0}. The higher area percentage of the ~445eV peak relative to the ~444eV peak, plotted in Figures 3c and 3d, show that RTA and FLA are both effective at

oxidizing indium back to In_2O_3. Table 1 shows the calculated values for all of the area percentages under the curves of the de-convoluted peaks in Figure 3. The similarity in the ~445eV to ~444eV peak area ratio in these spectra indicates that FLA was just as effective at oxidizing indium as RTA. Similarly, as shown in Figure 4, the relative area percentage under the curve of the ~486eV binding energy peak is a measure of the combined amount of reduced SnO and unoxidized Sn^{+0}. The extent to which tin was in the +4 oxidation state, as SnO_2, was indicated by the relative area percentage under the curve of the ~487eV peak to the ~486eV peak. As shown in Figure 4a, the ITO target granules have a significant amount of SnO_2. Figure 4b shows that EBPVD reduces much of this tin oxide to SnO and Sn^{+0}. RTA and FLA, as shown by the area percentage of the ~487eV peak relative to the ~486eV peak in Figures 4c and 4d, oxidizes much of this tin back to SnO_2. Table 2 shows the calculated values for all of the area percentages of the de-convoluted peaks in Figure 4. The higher ~487eV to ~486eV area ratio in these spectra indicates that FLA was more effective at oxidizing the tin component than RTA.

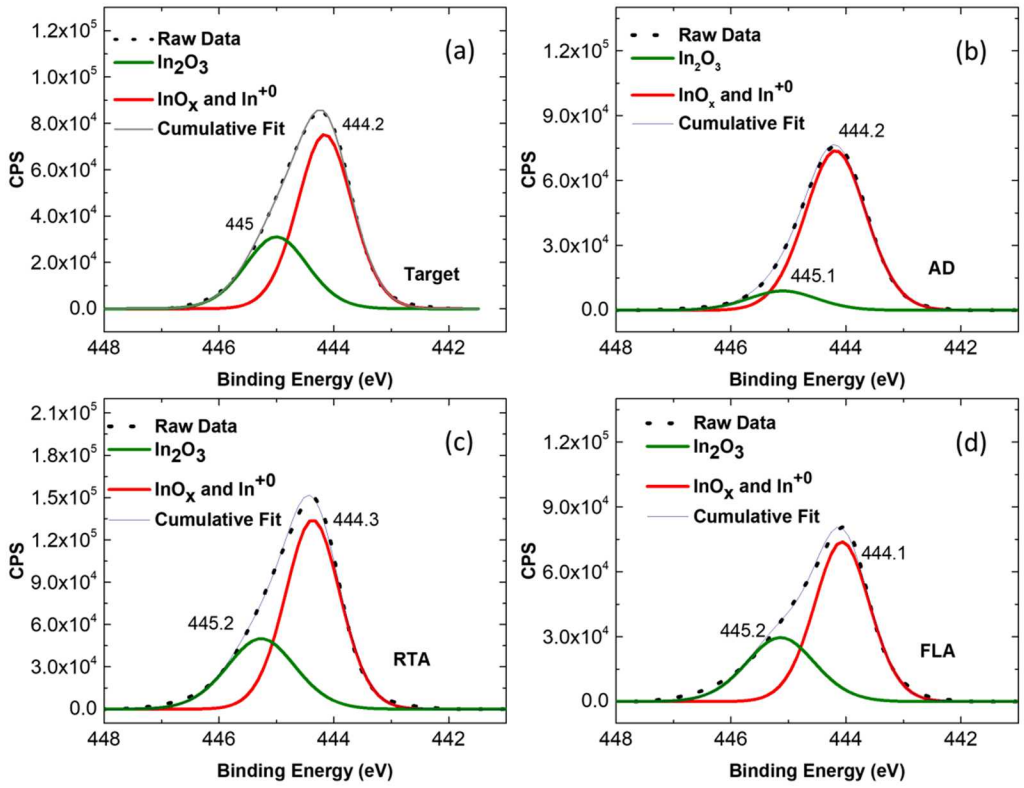

Fig. 3 In 3d XPS spectra for the (a) ITO target, (b) as deposited ITO, (c) RTA treated ITO, and (d) FLA treated ITO

Table 1 Relative peak area% for In 3d XPS spectra for the pre-deposited ITO target, AD, RT, and FLA treated ITO.

Formula	**In_2O_3**	**InO_x and In^{+0}**
Target (Area%)	32.0	68.0
AD (Area%)	12.0	88.0
RTA (Area%)	31.7	68.3
FLA (Area%)	33.0	67.0

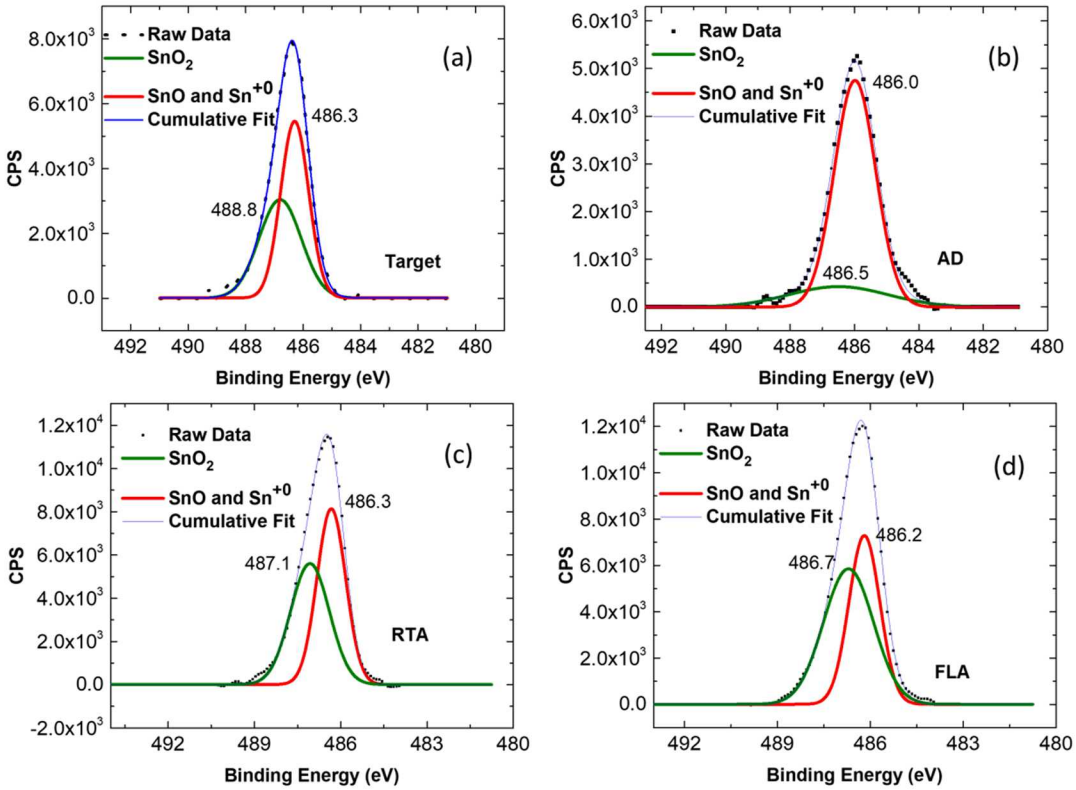

Fig. 4 Sn 3d XPS spectra for the (a) ITO target, (b) as deposited ITO, (c) RTA treated ITO, and (d) FLA treated ITO

Table 2 Relative peak area% for Sn3d XPS spectra for the pre-deposited ITO target, AD, RT, and FLA treated ITO.

Formula	**SnO_2**	**SnO and Sn^{+0}**
Target (Area%)	45.7	54.3
AD (Area%)	17.8	82.3
RTA (Area%)	48.2	51.8
FLA (Area%)	56.5	43.5

UV-Vis spectroscopy measurements, shown in Figure 5, quantify the extent annealing improves the visible transparency of the as deposited ITO thin film. The increased transparency of annealed ITO over unannealed ITO was consistent with the oxidation, detected by XPS, when an annealing process was applied. Annealing driven oxidation of the deposit improved its transparency by mitigating the presence of visibly opaque In^{+0}, by oxidizing it into non-stoichiometric InO_x, and blue shifting the absorbance of indium oxides present, to wavelengths outside the visible spectrum, specifically wavelengths shorter than 400nm, by oxidizing non-stoichiometric InO_x to In_2O_3 [18, 19]. Similarly, annealing driven oxidation mitigated the presence of visibly opaque Sn^{+0}, by oxidizing it to SnO, and blue shifting the absorbance of tin oxides present to wavelengths outside the visible spectrum, specifically ~500nm to ~256nm, by oxidizing SnO to SnO_2 [20].

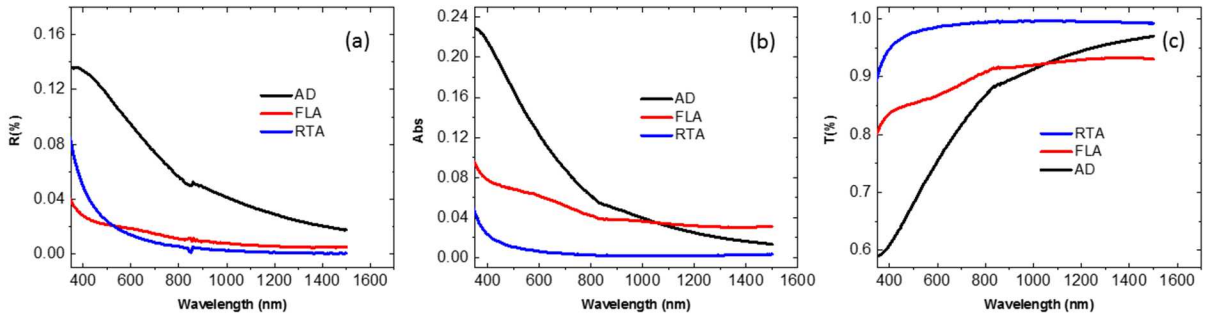

Fig. 5 Percent reflectance (a), absorbance (b), and percent transmission (c) of 200Å of ITO doped glass that was left amorphous in its as deposited state (AD), crystalized via FLA (FLA), and crystallized via RTA (RTA) from 375nm to 1600nm

Two conclusions could be made from the absorbance measurements collected using 632.8nm light directed through varying thicknesses of unannealed as deposited ITO and annealed ITO. First, increasing the thickness of the as deposited material can lower its extinction coefficient. Second, the extent the annealing processes applied in this study can establish visibly transparent thin films with uniform compositions was not significantly affected by the initial thickness of the as deposited film. As shown in Figure 6, assuming the transmittance and absorbance of the deposited material can be predicted with the Lambert Law ($T = e^{-\mu\ell}$), where $T =$ %transmission, $\mu =$ attenuation coefficient, and $\ell =$ absorbing thickness. According to the Sopra Materials Database, the extinction coefficient $\in$ at 632.8nm for typical ITO is 0.058. The attenuation coefficient was calculated using the equation $\mu = 4\pi \in/\lambda$, using $\lambda = 632.8$nm to give a μ value of $1.15\text{x}10^{-4}$Å^{-1}. The absorbing thickness ℓ was taken to be $\ell = Xt$, with the variable t being the thickness of the ITO and X being the percentage of reduced species, which is about 65% as calculated from the areas under the lower binding energy de-convoluted curves from the XPS for annealed ITO and about 87% for unannealed ITO. With a $1.15\text{x}10^{-4}$Å^{-1} attenuation coefficient for ITO, the absorbance of standard ITO is expected to increase by $1.15\text{x}10^{-4}$ with each additional angstrom of thickness. This differs significantly from unannealed as deposited ITO which initially has an attenuation coefficient of $3.04\text{x}10^{-3}$Å^{-1} but decreases to $1.76\text{x}10^{-3}$Å^{-1} as the thickness of the as deposited material was increased to 600Å. This suggests that the composition of the as deposited material changed to something more transparent as more of it was deposited. For RTA processed coatings, the attenuation coefficient for thicknesses up to

400Å stayed steady at 3.20×10^{-4} Å^{-1} and increased slightly to 3.32×10^{-4} Å^{-1} for thicknesses greater than 400Å. This shows that RTA is very effective at making the as deposited material transparent but loses some of this effectiveness for thicknesses above 400 angstroms. For FLA processed coatings, the attenuation coefficient for 200Å thickness is 2.03×10^{-3} per angstrom and decreases to 1.46×10^{-3} per angstrom as the thickness increases to 600Å. Though this was higher than the attenuation coefficients of RTA processed and standard ITO samples, its decrease is more similar to the as deposited material, though it does not drop as much and indicates that the effectiveness of FLA at driving reactions needed to make as deposited ITO transparent does not diminish with increasing initial thickness.

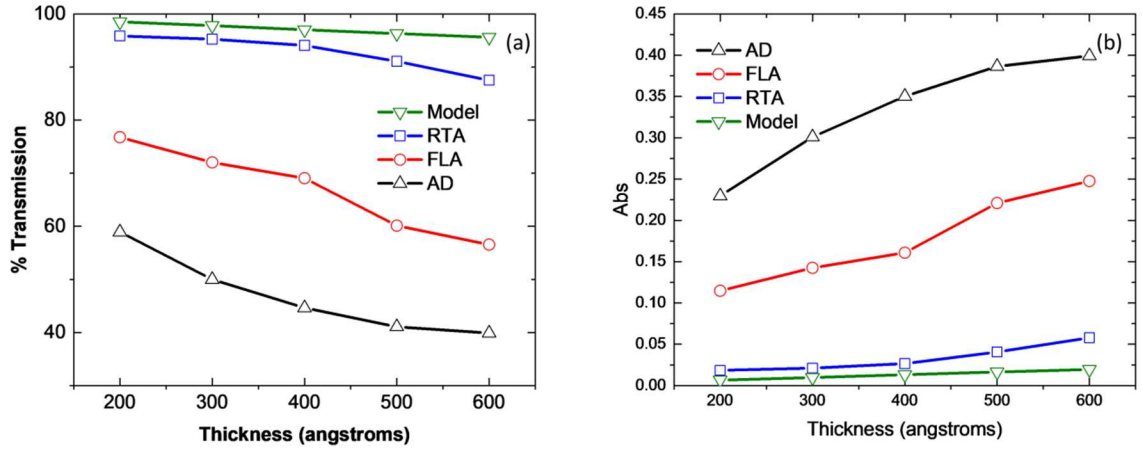

Fig. 6 632.8nm laser (a) % transmission and (b) absorbance of AD, RTA, and visible FLA ITO thin films compared with modelled optical properties of ITO (Abs is calculated as $log(1/T)$

4-point probe measurements, shown in Figure 7 for thicknesses up to 600Å, find that RTA and FLA processing are similarly effective at converting electrically insulating amorphous as deposited ITO films into electrically conductive thin films. As shown in Figure 8, the majority of the electrical resistivity decrease induced by FLA processing occurs after one FLA treatment. Repeating the FLA treatment can further reduce the electrical resistivity of the thin film, but its effect becomes negligible after approximately ten treatments. The similarity in electrical resistivity of RTA and FLA processed samples suggest that the composition of thin films prepared by both processes is also comparable. This agrees with the similarity of the XPS spectra

of the annealed ITO samples shown in Figures 3 and 4. This general correlation between increased transparency with increased electrical conductivity indicates that electrical resistivity measurements can be used to determine if an ITO annealing process was effective at establishing a visibly transparent electrically conductive thin film. Specifically, annealed ITO deposits that are more visibly transparent are generally more electrically conductive and more electrically conductive ITO is generally more visibly transparent.

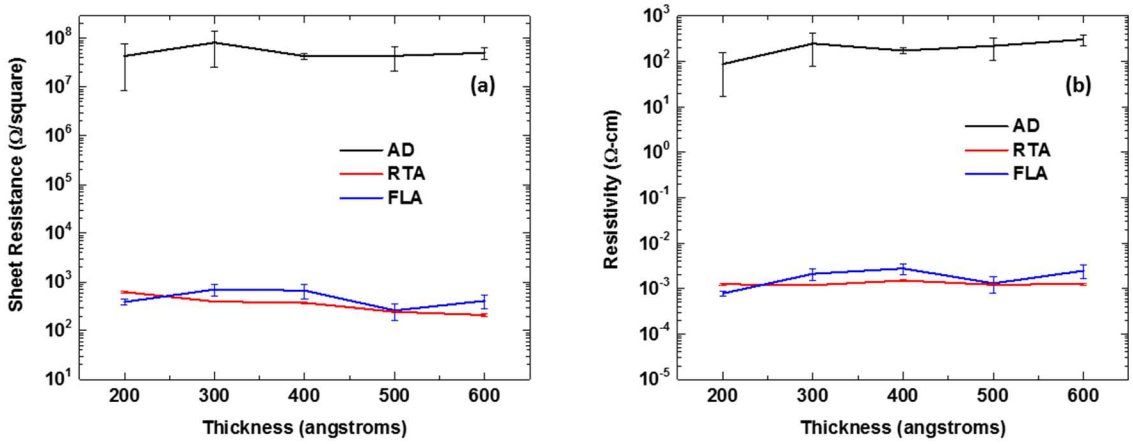

Fig. 7 (a) Sheet resistance and (b) resistivity of 200, 300, 400, 500, and 600 Å thick ITO on glass for AD, RTA, and FLA EBPVD samples

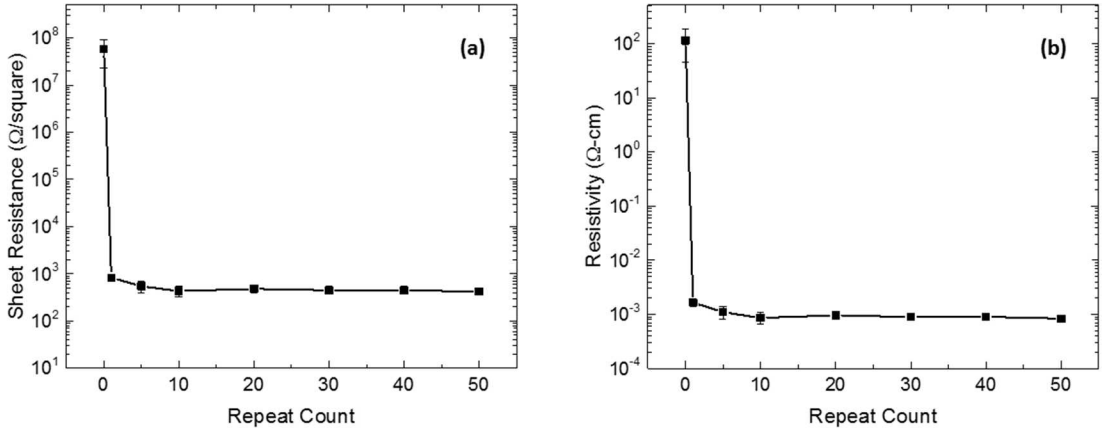

Fig. 8 (a) Sheet resistance and (b) resistivity of 200Å ITO films FLA treated with varying repeat counts

Assessing the XRD, XPS, UV/Vis, and sheet resistance data collected in this study, the visibly opaque nature of the electrically insulating reduced species in the as deposited ITO coatings and the visibly transparent nature of the electrically conductive oxidized species suggest that only visible light is needed to flash anneal amorphous ITO deposits into transparent electrically conductive films. This hypothesis is supported by data from selective filtering of the 200nm to 1500nm spectrum emitted by the Xe arc-lamp during the FLA process and assessing the electrical resistivity of the resulting samples. In this study, light with wavelengths from 200nm to 425nm was considered to be UV light, light with wavelengths from 425nm to 675nm was considered to be visible light, and light with wavelengths from 675nm to 1500nm was considered to be IR light. Details on which wavelengths of light impinged on the sample when different filters were applied are detailed in Table 3. The results show that FLA processing with visible light filtered out was ineffective at oxidizing amorphous ITO deposits into electrically conductive visibly transparent thin films. Moreover, exclusively using visible light in the FLA process (Vis-FLA) generated the most electrically conductive films, films that were even more electrically conductive than RTA generated films. Though the visible transparency of Vis-FLA processed as deposited ITO was still less than that of the RTA processed ITO, the improved electrical conductivity of Vis-FLA processed ITO suggests that UV and IR light may drive reactions that inhibit the formation of electrically conductive ITO. SEM images, shown in Figure 9, find that excessive unfiltered FLA treatments (specifically applying substantially more than the 20 FLA treatments applied in the typical FLA process used in this study) can cause significant ablative damage to the ITO surface. It is conceivable that UV light and IR light, relative to visible light, may preferentially drive this decomposition, as visibly transparent electrically conductive ITO is still opaque to UV and IR light.

Table 3: Sheet resistivity of FLA processed as deposited ITO using various spectral filters. Each FLA process consisted of 20 applications, conducted in series, of a pulse envelop consisting of 8 flashes of light. Consequently, each FLA process exposed the as deposited samples of ITO with 160 flashes of light. The resistivity of ITO is reported to be 7.5 x 10^{-4} Ω-cm [21]

Light	Description	Impinging Light During the Annealing	Resistivity (Ω-cm)	Electrically	Visibly

Filtered		Process		Conductive?	Transparent?
Vis-IR	Hot and cold mirrors placed in beam path	340nm to 425nm (Only UV impinging)	$5.0x10^{2} \pm 2.2x10^{2}$	No	No
Vis	Cold mirror	340nm to 425nm and 675nm to 1500nm (UV and IR light impinging)	$5.5x10^{2} \pm 3.1x10^{2}$	No	No
AD	None. This is the unannealed sample. It is listed as a reference	None (UV, Vis, and IR light impinging)	$1.2x10^{2} \pm 2.2x10^{1}$	No	No
UV-Vis	Cerium oxide filter with cold mirror in the beam path	675nm to 1200nm (Only IR light impinging)	$7.9x10^{2} \pm 2.9x10^{2}$	No	No
UV-Vis-IR	Hot mirror, cerium oxide filter, and cold mirror in the beam path	None, all light filtered	$5.5x10^{2} \pm 1.7x10^{2}$	No	No
UV	Cerium oxide filter in the beam path	425nm to 1500nm (Vis and IR light impinging)	$1.1x10^{-3} \pm 1.4x10^{-4}$	Yes	Yes
IR	Hot mirror in the beam path	340nm to 700nm (UV and visible light impinging)	$1.1x10^{-2} \pm 6.6x10^{-3}$	Yes	Yes
No filters	No filters in the beam path	200nm to 1500nm (UV, Vis, and IR light impinging)	$6.6x10^{-3} \pm 3.3x10^{-3}$	Yes	Yes
UV-IR	Cerium oxide filter and hot mirror in the beam path	425nm to 700nm (Only Vis light impinging)	$7.3x10^{-4} \pm 1.0x10^{-4}$	Yes	Yes
RTA	No filters. Sample is baked in an oven.	None	$1.2x10^{-3} \pm 7.4x10^{-5}$	Yes	Yes

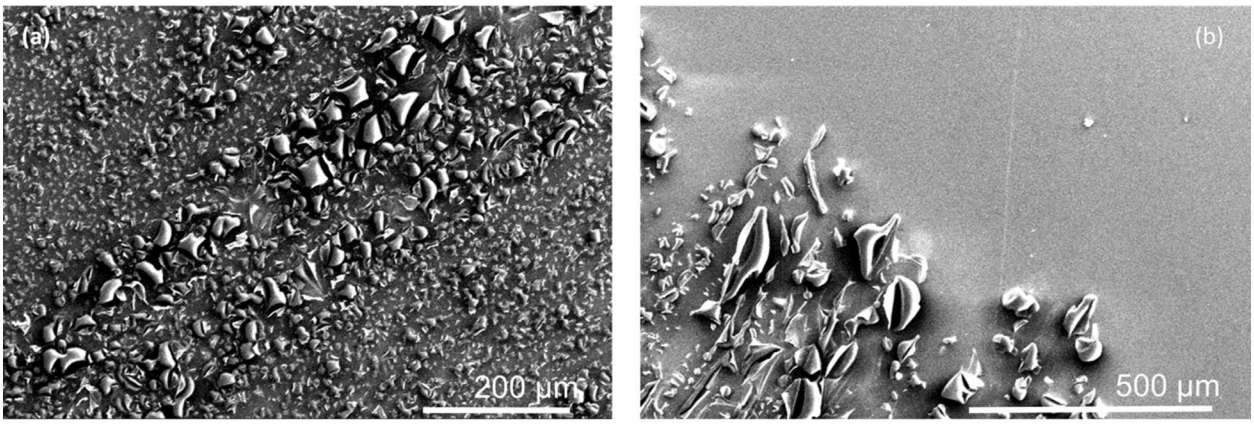

Fig. 9 SEM images of 200Å of ablated ITO for (a) FLA region and (b) intersection between FLA region and smooth unannealed ITO

A review of all the data collected in this study suggest that the FLA process creates visibly transparent electrically conductive ITO thin films out of visibly opaque electronically insulating as deposited ITO in the following manner. ITO that is vapor deposited on a glass substrate consists of an amorphous film largely made of visible light absorbing In^{+0} and InO_x. Embedded within these indium species is the appropriate distribution of visible light absorbing Sn^{+0} and SnO to allow the formation of electrically conductive visibly transparent ITO, specifically, polycrystalline In_2O_3 doped with ~10wt% SnO_2. Visible light initially flashed during the FLA process is locally absorbed by the metals and partially oxidized species present. This absorption excites these species and their subsequent vibrational relaxation locally heats the deposit where these reduced species are located [22, 23]. This heat then drives oxidation and crystallization reactions wherein small grains begin to grow at the nucleation sites, as visibly opaque In^{+0} and InO_x are crystallized into visibly transparent In_2O_3, and visibly opaque Sn^{+0} and SnO are crystallized into visibly transparent SnO_2. The distribution of SnO_2 in the ITO film allows it to integrate with In_2O_3 to form SnO_2 doped In_2O_3. This n-doping imparts electrical conductivity to this polycrystalline amalgamation as electrons from the integrated tin can populate the conduction band of the In_2O_3 crystal [24]. Since incompletely oxidized species are scattered throughout the amorphous deposit, localized heating would simultaneously initiate ITO grain nucleation sites randomly distributed throughout the deposit. Subsequent flashes of visible light are absorbed by any remaining incompletely oxidized species in the amorphous regions, in

the process creating additional grains while propagating reasonably unperturbed through the fully oxidized visibly transparent SnO_2 doped In_2O_3. Since the additional flashes only cause heating in the amorphous regions of the film deposit, the population of small grains can increase within the amorphous regions, but because the visible light passes through the previously formed grains, they likely do not get hot enough to increase in size. Nascent ITO crystals in the as deposited material will not have a preferential initial orientation so it is expected that these nascent crystals will all have random orientations. This makes it unlikely than any of these nascent crystals will merge with other ITO crystals in the deposit as FLA induced crystal growth continues.

In contrast, during RTA the grains continually receive uniform heating and are therefore more likely to grow larger in size, as both of the grains and amorphous regions are sufficiently heated continually and the atoms have more time to migrate through the media. The slightly narrower (200) peak on the RTA XRD curve from Figure 2 indicates larger grain size in the RTA treated ITO. The more uniform, continuous heating throughout the entire film is likely the cause of the better transmission properties that result from the RTA treated film over that of the localized non-uniform heating of the FLA treated film.

While UV and IR light could also be used to drive the desired crystallizing oxidation, it is preferable to use visible light since annealed ITO can still continue absorbing UV and IR light even after it has been oxidized and crystallized. This can reduce the intensity of subsequent light pulses applied to oxidize and crystallize any remaining incompletely oxidized species in the deposit. Additionally, the capability of the desired visibly transparent electrically conductive ITO to absorb UV and IR light can lead to undesired photo decompositions or ablations. Such damage can reduce both the electrical conductivity and visible transparency of the annealed ITO by introducing optical defects in the film.

Conclusions

FLA with visible light has been found to be an effective technique to prepare visibly transparent electrically conductive ITO coatings more quickly and with less thermal stress than conventional annealing techniques such as RTA. The speed at which it is possible to complete FLA processing of ITO with pulsed, high intensity visible light and the reduced overall heating of the target substrate arises from the selective heating of reduced Sn^{+0}, In^{+0}, SnO, and InO_x appropriately distributed in the as deposited ITO films to drive their crystallization into electrically conductive visibly transparent tin doped In_2O_3. Use of visible light is crucial to this process since it can be absorbed to anneal the visibly opaque and electrically insulating incompletely oxidized indium and tin in the as deposited ITO while propagating freely and thus not perturbing the visibly transparent and electrically conductive tin doped In_2O_3 that is initially present or generated by FLA. This suggests visible light based FLA can be a promising approach for establishing transparent electrically conductive ITO coatings on thermally sensitive visibly transparent substrates, like polymers, since visible light will not interact with or heat such substrates. UV and IR light are not effective for driving an FLA process to create ITO based visibly transparent electrical conductors since both these regions of light can be absorbed by annealed ITO. This can lead to undesired thermal decomposition or ablation of the electrically conductive visibly transparent tin doped In_2O_3 the FLA process was applied to produce.

The drawback in applying a visible light based FLA process to create electrically conductive visibly transparent tin doped In_2O_3 thin films, from ITO deposited using EBPVD, is that such films are not as transparent as films prepared with conventional thermal annealing techniques, but what's gained is faster processing time and avoidable thermal stress to visibly transparent substrates that may not survive the homogenous heating imparted from RTA, such as visibly transparent polymers.

Acknowledgements

Partial support for this work was provided by AFRL through the Space Dynamics Laboratory, Utah State University, via subcontract HQ0147-11-D-0052-0031 to the University of New Mexico (RAK). Useful discussions with Professor Sang E. Han and Mr. Rafal Dziedzic are gratefully acknowledged. Sandia National Laboratories is a multi-mission laboratory managed and operated by National Technology and Engineering Solutions of Sandia, LLC., a wholly owned subsidiary of Honeywell International, Inc., for the U.S. Department of Energy's National Nuclear Security Administration under contract DE-NA0003525.

The authors declare no competing interest or conflict of interest in the publication of this article.

ORCID John B. Plumley: 0000-0002-6404-2467

ORCID Adam W. Cook: 0000-0003-0695-1520.

ORCID Christopher A. Larsen: 0000-0003-0286-5545

ORCID Kateryna Artyushkova: 0000-0002-2611-0422

ORCID Sang M. Han: 0000-0002-1008-1700

ORCID Thomas L. Peng: 0000-0002-9369-5715

ORCID Richard A. Kemp: 0000-0002-2063-3812

References

[1] Hecht DS, Hu LB, Irvin G (2011) Emerging transparent electrodes based on thin films of carbon nanotubes, graphene, and metallic nanostructures. Adv. Mater. 23: 1482-1513

[2] Fortunato E, Ginley D, Hosono H, Paine DC (2007) Transparent conducting oxides for photovoltaics.MRS Bull. 32: 242-247

[3] Lin CW, Chen HI, Chen TY, Huang CC, Hsu CS, Liu WC (2011) Ammonia sensing characteristics of sputtered indium tin oxide (ITO) thin films on quartz and sapphire substrates. IEEE Trans. Electron Devices 58: 4407-4413

[4] Habibi MH, Talebian N (2005) The effect of annealing on structural, optical and electrical properties of nanostructured tin doped indium oxide thin films. Acta Chimica Slovenica 52: 53-59

[5] Szkutnik PD, Rapenne L, Roussel H, et al. (2013) Influence of precursor nature on the thermal growth of tin-indium oxide layers by MOCVD. Surf. Coat. Technol. 230: 305-311

[6] Kim H, Gilmore CM, Pique A, et al. (1999) Electrical, optical, and structural properties of indium-tin-oxide thin films for organic light-emitting devices.J. Appl. Phys. 86: 6451-6461.

[7] Stoica TF, Gartner M, Stoica T, et al. (2005) Properties of high-porosity sol-gel derived indium-tin oxide films.J. Optoelectron. Adv. Mater. 7: 2353-2358.

[8] Ito D, Masuko K, Weintraub BA, McKenzie LC, Hutchison JE (2012) Convenient preparation of ITO nanoparticles inks for transparent conductive thin films. J. Nanopart. Res. 14: 1-7

[9] Manavizadeh N, Khodayari A, Soleimani EA, Bagherzadeh S, Maleki MH (2009) Structural Properties of Post Annealed ITO Thin Films at Different Temperatures. Iran J. Chem. Chem. Eng.-Int. Engl. Ed. 28: 57-61.

[10] Gartner M, Stroescu H, Marin A, et al. (2014) Effect of nitrogen incorporation on the structural, optical and dielectric properties of reactive sputter grown ITO films. Appl. Surf. Sci. 313: 311-319.

[11] Noh M, Seo I, Park J, et al. (2016) Spectroscopic ellipsometry investigation on the excimer laser annealed indium thin oxide sol-gel films. Curr. Appl. Phys. 16: 145-149

[12] Kim Y, Park S, Kim BK, Kim HJ, Hwang JH (2015) Xe-arc flash annealing of indium tin oxide thin-films prepared on glass backplanes. Int. J. Heat Mass Transf. 91: 543-551

[13] Weller S, Junghähnel M (2015) Flash Lamp Annealing of ITO thin films on ultra-thin glass. Vak. in Forsch. Prax. 27: 29-33

[14] Kang Y, Potnis T, El-Helw S, Liu T, Orlowski M (2013) in Mustain W, Chen F, Leonte O (eds) Nanotechnology.Electrochemical Soc Inc, Pennington

[15] Powder Diffraction File No. 06-0416 ICfDD,

[16] Al-Dahoudi N, Bisht H, Gobbert C, Krajewski T, Aegerter MA (2001) Transparent conducting, anti-static and anti-static-anti-glare coatings on plastic substrates. Thin Solid Films 392: 299-304

[17] Nelson AJ, Aharoni H (1987) X-ray photoelectron-spectroscopy investigation of ion-beam sputtered indium tin oxide-films as a function of oygen-pressure during deposition. J. Vac. Sci., A-Vacuum Surfaces and Films 5: 231-233

[18] Huang S, Ou G, Cheng J, Li H, Pan W (2013) Ultrasensitive visible light photoresponse and electrical transportation properties of nonstoichiometric indium oxide nanowire arrays by electrospinning. J. Mater. Chem. C 1: 6463-6473

[19] Xu R, Li H, Zhang W, et al. (2016) The fabrication of In2O3/In2S3/Ag nanocubes for efficient photoelectrochemical water splitting. PCCP 18: 2710-2717

[20] Sinha AK, Manna PK, Pradhan M, Mondal C, Yusuf SM, Pal T (2014) Tin oxide with a p-n heterojunction ensures both UV and visible light photocatalytic activity. RSC Adv. 4: 208-211.

[21] Farhan MS, Zalnezhad E, Bushroa AR, Sarhan AAD (2013) Electrical and optical properties of indium-tin oxide (ITO) films by ion-assisted deposition (IAD) at room temperature. Int. J. Precis. Eng. Manuf. 14: 1465-1469.

[22] Beard MC, Midgett AG, Hanna MC, Luther JM, Hughes BK, Nozik AJ (2010) Comparing multiple exciton generation in quantum dots to impact ionization in bulk semiconductors: implications for enhancement of solar energy conversion. Nano Letters 10: 3019-3027

[23] Bricker WP, Shenai PM, Ghosh A, et al. (2015) Non-radiative relaxation of photoexcited chlorophylls: theoretical and experimental study. Sci. Rep. 5: 13625 (https://www.nature.com/articles/srep13625) Accessed 7 February 2018

[24] Edwards PP, Porch A, Jones MO, Morgan DV, Perks RM (2004) Basic materials physics of transparent conducting oxides. Dalton Trans.: 2995-3002.

Sandia National Laboratories is a multimission laboratory managed and operated by National Technology & Engineering Solutions of Sandia, LLC, a wholly owned subsidiary of Honeywell International Inc., for the U.S. Department of Energy's National Nuclear Security Administration under contract DE-NA0003525.